Achromatic Cascade Optical System with Hybrid Lenses for Distortion-compensated Multifocusing of Ultrashort Pulse Beams

Jun Amako and Hidetoshi Nakano
Faculty of Science and Engineering, Toyo University, 2100 Kujirai, Kawagoe, Saitama 350-8585, Japan

Keywords: Ultrafast Optics, Diffractive Optics, Hybrid Lens, Systems Design.

Abstract: We report an achromatic cascade optical system for multifocusing ultrashort pulse beams in its application in high-precision materials processing. The challenge is to eliminate the beam-radius-dependent pulse broadening or pulse front distortion from the arrayed pulses. We propose the inclusion of a pair of hybrid refractive-diffractive lenses for chromatic aberration correction and dispersion management in the system. From numerical analysis, we have realized that the hybridized system has enormous potential to improve not only the spatial resolution but also the temporal resolution to their respective limits in generating arrayed pulse beams. This pulse delivery system enables high-throughput material processing using ultrashort-pulsed lasers.

1 INTRODUCTION

There has been growing interest in ultrashort-pulsed laser for precision manufacturing. The deterministic and reproducible nature of ultrashort pulses in light-matter interaction is indispensable for micro and nano-machining without thermal damages (Lenzner et al, 1999; Chimier et al, 2011). On the other hand, a material can be processed at multiple points simultaneously with arrayed pulse beams to obtain a high throughput. For arrayed irradiation, diffractive beam splitters (DBSs) are extensively used with nanosecond-pulsed lasers for a variety of laser-based processes (Amako and Fujii, 2016).

A diffracted ultrashort pulse suffers chromatic aberrations, however, due to its broad spectrum, resulting in spatial and temporal pulse lengthening. Such pulse broadening can be ignored by diffracting and focusing the pulses near the optical axis but the severely limited work areas remain challenging (Kuroiwa et al, 2004; Hayasaki et al, 2005; Kelemen et al, 2007; Sakakura et al, 2009; Jesacher and Booth, 2010). Although several efforts have been made to fix the pulse distortions, temporal broadening remains unfixed (Amako et al, 2002; Li et al, 2005; Hasegawa and Hayasaki, 2014). Minguez-Vega et al. proposed a diffractive-refractive lens triplet for simultaneous compensation of spatio-temporal pulse distortions (Minguez-Vega et al, 2006). Multifocusing performance of the triplet was evaluated in optical experiments (Martinez-Cuenca et al, 2012; Torres-Peiro et al, 2013). According to their report, it was the temporal distortion rather than the spatial distortion restricting the outer-most angle of pulse diffraction or the length of the beam array, which determines the process throughput.

These prior studies motivated us to explore a simple and practical method to design a pulse delivery system for multifocusing ultrashort pulse beams. We conceptualized a novel achromatic cascade system, designed a prototype, and proved its operation principle with 20-fs-pulses (Amako and Nakano, 2018). Yet beam-diameter-dependent pulse broadening or pulse front distortion was detected in the transmitted pulses. These temporal distortions can be minimized by narrowing the beam diameter, but sacrificing the spatial resolution. Such parabolic distortions are present due to the group-velocity dispersions in the refractive lenses used in the system and cannot be compensated by the action of refractive lenses alone. Instead of refractive lenses, hybrid lenses composed of a refractive and diffractive surface can be employed for chromatic aberration correction and dispersion management (Stone and George, 1988; Piestun and Miller, 2001). We here report on "hybridization" of the cascade system for distortion-free multifocusing ultrashort pulses.

Amako, J. and Nakano, H.
Achromatic Cascade Optical System with Hybrid Lenses for Distortion-compensated Multifocusing of Ultrashort Pulse Beams.
DOI: 10.5220/0007470202410247
In *Proceedings of the 7th International Conference on Photonics, Optics and Laser Technology (PHOTOPTICS 2019)*, pages 241-247
ISBN: 978-989-758-364-3
Copyright © 2019 by SCITEPRESS – Science and Technology Publications, Lda. All rights reserved

2 PROTOTYPE CONCEPT

Figure 1 shows the schematic of the prototype cascade optical system. The diffractive subsystem consists of a diffractive beam splitter (DBS) and a diffractive lens (DL) of positive focal length. The refractive subsystem, which is afocal, has a pair of refractive lenses L_1 and L_2 with positive focal lengths. These two subsystems are cascaded and a phase plate (PP) is placed between them. Upon entering the system, an ultrashort pulse beam is divided by the DBS, producing a large angular dispersion. This dispersion is the origin of chromatic aberrations, which distorts the beam spot and stretches the pulse.

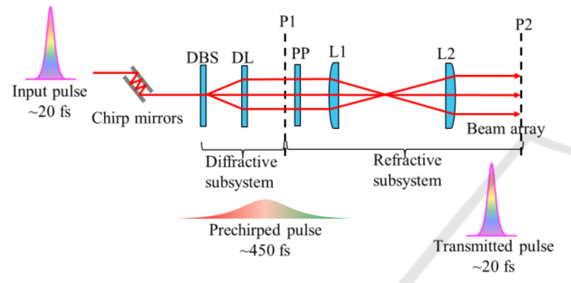

Figure 1: Schematic configuration of the prototype cascade system: DBS; diffractive beam splitter, DL; diffractive lens, PP; phase plate, L_1, L_2; refractive lenses. P_1, P_2 are the intermediate plane and exit plane, respectively.

Achromaticity of the system is the key to simultaneous compensation of the spatio-temporal pulse distortions. The diffractive subsystem is designed to correct the lateral chromatic aberrations; it forms an array of spatially identical pulse beams at the intermediate plane, P_1. The phase plate (PP) eliminates the angular dispersions of the diffracted pulse beams. The refractive subsystem is designed to correct the longitudinal chromatic aberrations; it generates an array of spatio-temporally identical pulse beams at the exit plane P_2, which is the work area. Group delay dispersions primarily caused by the refractive subsystem can be compensated for by prechirping the input pulse and therefore, the focused pulse at P_2 can be compressed back to the initial pulse duration.

3 REMAINING ISSUE

For proof-of-principle, we designed a prototype system and evaluated it with 20-fs-pulses by characterizing the transmitted pulses at P_2. In this prototype, two lenses in the afocal subsystem were made from E-FDS3 (HOYA), which was highly dispersive with ν_d = 17: ν_d is the Abbe number (HOYA's Official Website). Figure 2 shows the focused beam widths plotted against detection positions for the diffraction angles of 0.0º, 1.7º and 2.9º. The solid line in the figure represents the theoretically predicted beam widths for a Gaussian beam with no aberrations (M^2 = 1). The pulse beams on-axis and off-axis were tightly focused to a diffraction limit, 20 µm, at the focal point. From these results, we state that the cascade system is able to correct chromatic aberrations introduced in the diffracted 20-fs-pulse beams.

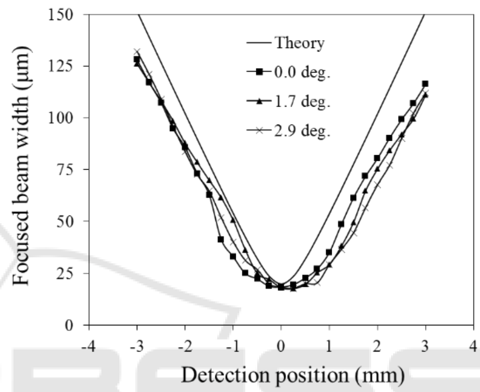

Figure 2: Focused beam widths vs. detection position. Solid line represents a theoretical prediction and plots are the measured data.

Another crucial issue in the prototype system can be identified in the time domain. Figure 3 shows the autocorrelation signals obtained from (a) the input pulse, (b) the focused pulse at P_2 in the prototype with two E-FDS3 refractive lenses, and (c) the transmitted pulse through an 8.0-mm-thick parallel plate of E-FDS3. The signal in Fig. 3(c) was obtained by focusing the pulse with a parabolic mirror. The plate thickness was set equal to the total thickness of two refractive lenses. On comparing these signals, we observed some distinctions: The input pulse width was 22 fs, the pulse width at the exit of the system was 35 fs, and the pulse width after the parallel plate was 24 fs. In addition, ripple structures were seen on the pedestal in Fig. 3(b). Through this observation, we understand that the temporal distortions in Fig. 3(b) were due to the group-velocity dispersions in the lenses, which introduced beam-radius-dependent pulse broadening or pulse front distortion.

Pulse front distortion, which is in proportion to the square of the beam radius, is given by

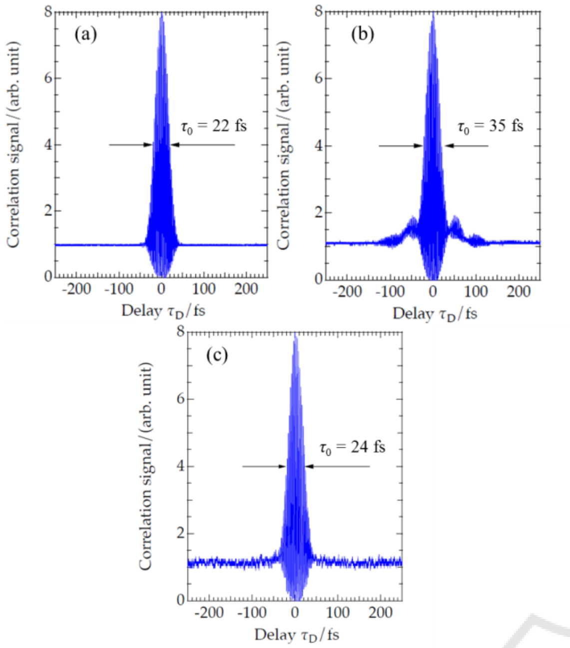

Figure 3: Auto-correlation signals obtained (a) from the input pulse, (b) from transmitted pulse at P_2 in the cascade system with the E-FDS3 refractive lenses, and (c) from the transmitted pulse after the E-FDS3 parallel plate.

$$\Delta\tau = \frac{\lambda_0}{n_0 - 1}\frac{\mathrm{d}}{\mathrm{d}\lambda}\left(\frac{\mathrm{dn}}{\mathrm{d}\lambda}\right)\frac{R^2}{cf_0}\Delta\lambda \qquad (1)$$

where λ_0 is the center wavelength, $\Delta\lambda$ is the wavelength bandwidth, $n(\lambda)$ is the refractive index of the lens glass, f_0 is the lens focal length at λ_0, R is the beam radius in the afocal system, and c is the speed of light in vacuum. For a transform-limited pulse, $\Delta\lambda\tau_0 = 0.441\lambda_0^2/c$, where τ_0 is the full width at half maximum (FWHM) of the pulse (Diels and Rudolph, 2006). As illustrated by Eq. (1), the distortion $\Delta\tau$ is inversely proportional to τ_0. Computed distortions are plotted against the beam radius in Fig. 4. The estimated distortion from the signal in Fig. 3(b) is 27 fs, as plotted in Fig. 4, where λ_0 = 780 nm, $\Delta\lambda$ = ±23 nm, n_0 = 2.066 at λ_0, f_0 = 278 mm at λ_0, $\mathrm{d}/\lambda(\mathrm{d}n/\mathrm{d}\lambda)$ = 0.4885 μm^{-2} at λ_0, and R = 11.7 mm. Given temporal distortions, the pulse width at P_2 can be estimated as $= \sqrt{\tau_0{}^2 + \Delta\tau^2}$. Distortions may be negligible for a 100-fs pulse but need to be addressed for a 20-fs pulse.

In order to eliminate such beam-radius-dependent temporal distortions, the dispersion management in the afocal subsystem is indispensable. For that purpose, we have considered a hybrid lens, which consists of a refractive lens and a diffractive lens. As is well known, a combination

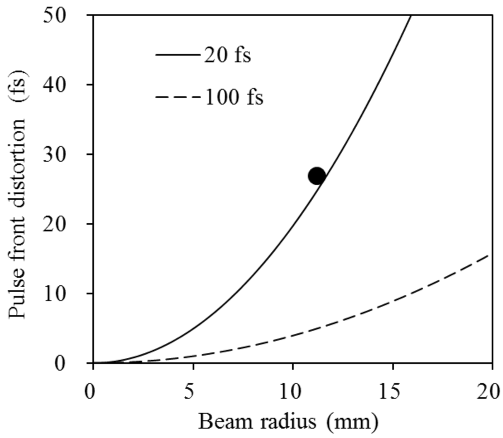

Figure 4: Computed pulse front distortions as a function of beam radius in the afocal subsystem.

of two types of lenses can correct longitudinal chromatic aberrations at the focus because the aberrations presented by the two lenses are opposite in sign. Likewise, two types of lenses, with appropriate physical parameters, can get the phase front and pulse front to coincide and further remove the parabolic temporal distortions. There is a temporal delay in the pulse front from the phase front after passing through the refractive lens, whereas the pulse front advances the phase front after passing through the diffractive lens.

Although the wavelength dependence of diffraction efficiency slightly narrows the spectral profile of a pulse, for a 20-fs-pulse the pulse width is scarcely affected.

4 SYSTEMS DESIGN

In design of the cascade system, the following two conditions need to be satisfied at P_2. Equation (1) needs to be accepted to correct longitudinal achromatic aberrations and Eq. (2) should be honored to compensate for pulse front dispersions. The two equations have some terms in common through which space and time are entangled:

$$\Delta z = \left[-\frac{f_{d0}}{\lambda_0} + 2\frac{\mathrm{d}F}{\mathrm{d}\lambda}\right]\Delta\lambda = 0 \qquad (2)$$

$$\Delta\tau = \left[-\frac{f_{d0}}{\lambda_0} + 2\frac{\mathrm{d}F}{\mathrm{d}\lambda} + 2\lambda_0\frac{\mathrm{d}}{\mathrm{d}\lambda}\left(\frac{\mathrm{d}F}{\mathrm{d}\lambda}\right)\right]\frac{R^2}{2cF_0{}^2}\Delta\lambda = 0 \qquad (3)$$

where f_d is the focal length of the diffractive lens and F is the focal length of the hybrid lens. Equation (1)

SCITEPRESS SCIENCE AND TECHNOLOGY PUBLICATIONS

was derived by using the ray matrix (Yariv and Yeh, 2003) of the cascade system and Eq. (2) was derived by applying an analytical model of pulse propagation time (Bor, 1988; 1989) to the system. Formula derivation was performed in a paraxial regime. Equations (2) and (3) hold for the off-axis beams as well as the on-axis beam, under first-order approximation.

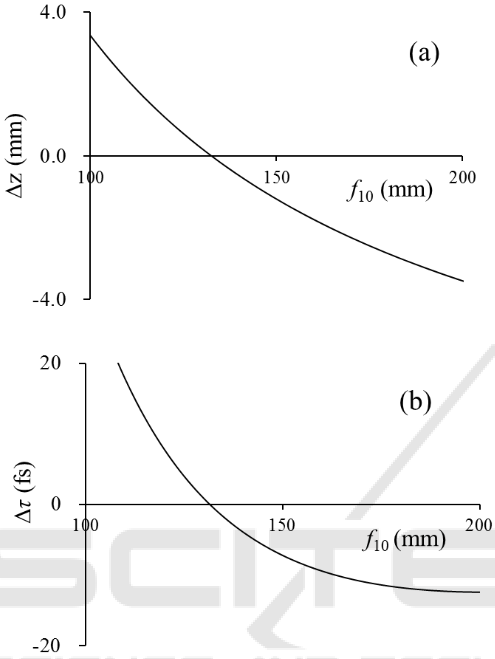

Figure 5: (a) Computed chromatic aberration and (b) computed pulse front distortion plotted against f_{10}, the refractive focal length of the hybrid lens to be designed.

For a focal length F to satisfy the above conditions, $\mathrm{d}F/\mathrm{d}\lambda$ needs to be a positive constant and $\mathrm{d}/\lambda(\mathrm{d}F/\mathrm{d}\lambda)$ needs to be zero across the spectral band of the pulse. Provided that the focal lengths of the refractive and diffractive lenses are $f_1(\lambda)$ and $f_2(\lambda)$, respectively, $F(\lambda)$ can be expressed as $F = f_1f_2/(f_1 + f_2)$, where the two lenses are assumed to be sufficiently thin. $f_1(\lambda)$ and $f_2(\lambda)$ are defined by $f_1(\lambda) = f_{10}\frac{n(\lambda)-1}{n(\lambda_0)-1}$ and $f_2(\lambda) = f_{20}\frac{\lambda_0}{\lambda}$, where the subscript 0 represents the focal length at λ_0. If the focal length f_{10} is picked as the design variable, the aberration can be zero at one focal length and the pulse front distortion can be zero at another focal length, as shown in Fig. 5. These two focal lengths should match; this condition can be attained by selecting a type of glass with a low dispersion degree or a high Abbe number.

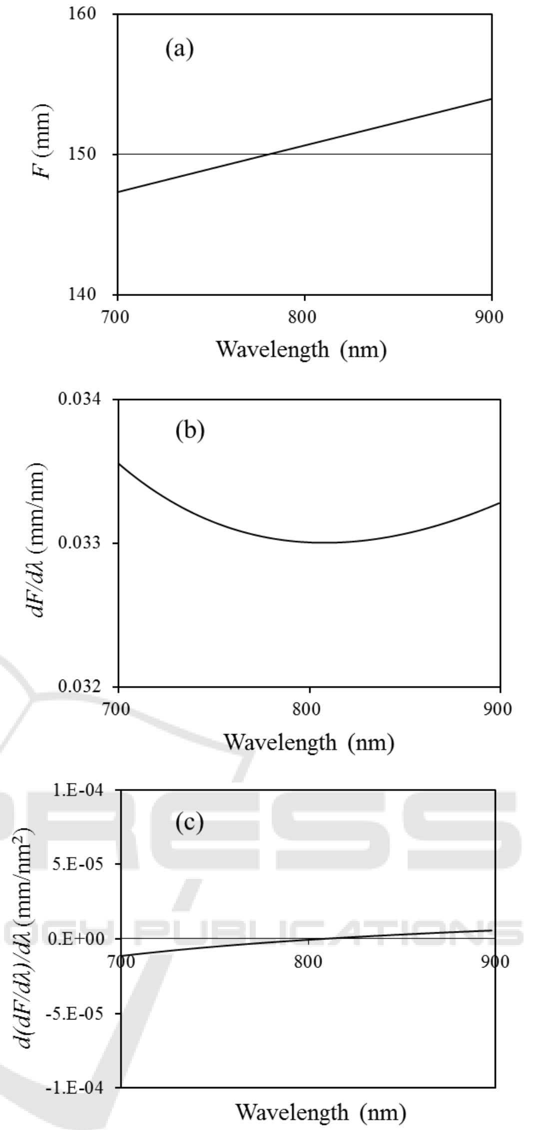

Figure 6: Dispersion properties of a designed hybrid lens. (a) Focal length F, (b) first derivative of F, and (c) second derivative of F plotted against wavelength, respectively.

5 RESULTS AND DISCUSSIONS

Assuming a pulse width of τ_0 = 20 fs with λ_0 = 780 nm and $\Delta\lambda$ = ±23 nm, we searched for a focal length F, which satisfies both the conditions (1) and (2), by scanning the focal length f_{10}. Other set conditions were the incident beam width of 5.0 mm ($2R$ = 15 mm), f_{d0} = 50 mm, and F_0 = 150 mm. As an example, when fused silica (ν_d = 69) is selected as lens material, we found f_{10} = 133 mm and f_{20} = −1144 mm for Δz = 0.0 mm using Eq. (2); we computed $\Delta\tau$ =

SCITEPRESS SCIENCE AND TECHNOLOGY PUBLICATIONS

0.87 fs and then τ = 20 fs from Eq. (3). The effective Abbe number (Harm et al, 2014) of this hybrid lens was calculated as 18. Figure 6 shows the dispersion properties of the designed hybrid lens. F, $\mathrm{d}F/\mathrm{d}\lambda$, and $\mathrm{d}/\lambda(\mathrm{d}F/\mathrm{d}\lambda)$ are plotted as a function of wavelength in Fig. 6 (a), (b), and (c), respectively. As illustrated by Fig. 6 (b), $\mathrm{d}F/\mathrm{d}\lambda$ has a minimum in the spectral range of the pulse. Accordingly, $\mathrm{d}/\lambda(\mathrm{d}F/\mathrm{d}\lambda)$ comes close to zero around the center wavelength of the pulse, thus nearly eliminating the pulse front distortions for Δz = 0, as is seen from Eq. (3).

In the prototype, a pair of refractive lenses made from E-FDS3 (ν_d = 17) were employed, for which we found $F_0 = f_{10}$ = 278 mm ($f_{20} = \infty$) for Δz = 0.0 mm using Eq. (2) and we obtained $\Delta\tau$ = 39 fs with $2R$ = 28 mm and thus τ = 44 fs using Eq. (3).

In this example design, there was a small gap between the two f_{10} values: one for zero aberration and the other for zero distortion. That gap was filled by selecting a type of glass that much less dispersive than fused silica, for example, FCD100 with ν_d = 95, further reducing the temporal distortion $\Delta\tau$. However, we preferred to use fused silica because of its compatibility with dry-etching processes that we would rely on in fabrication of the diffractive surface of a hybrid lens.

To verify the effects of the designed hybrid lens, we conducted numerical analysis to study the behaviors of the transmitted pulse. Computed focal position deviations or longitudinal chromatic aberrations at P_2 are plotted against the wavelength in Fig. 7. The aberrations were computed by applying the ray matrix of the cascade system. The designed hybrid lens with 150-mm-focal length allowed the transmitted pulse to focus at P_2 with a deviation of 40 μm across the wavelength range of 780 nm ± 23 nm (solid line). In contrast, a refractive singlet made from fused silica presented a lot of longitudinal aberrations with a deviation of ±1.2 mm across the wavelength range of interest (broken line).

Further, computed pulse front distortions are plotted against the beam radius in Fig. 8. Distortions were computed using Eq. (3). Employing a pair of the designed hybrids kept the distortions sufficiently small with increasing beam radius (solid line), whereas employing a pair of the refractive lenses made using E-FDS3 increased the distortions with increasing beam radius (broken line).

From these results, we conclude that the hybrid lens is able to compensate for spatio-temporal distortions introduced by splitting and focusing ultrashort pulse beams. In addition, a large diffractive dispersion inherent in a hybrid, lens offers a small footprint of

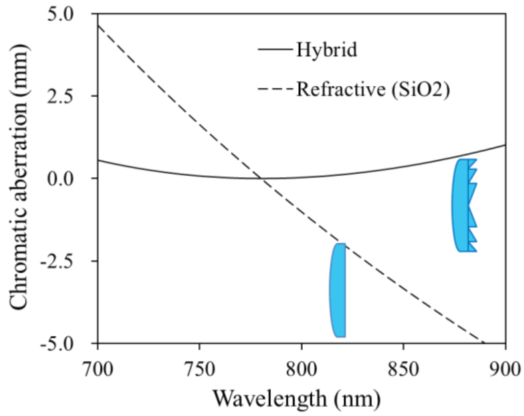

Figure 7: Computed chromatic aberrations at P_2 (in Fig. 1) against the wavelength. Solid line is for the cascade system with the designed hybrid lenses and broken line is for the cascade system with the fused silica refractive lenses.

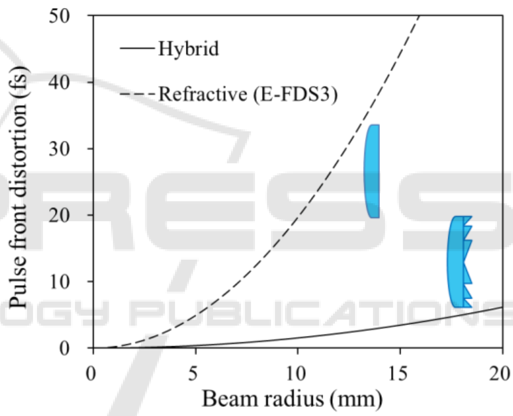

Figure 8: Computed pulse front distortions at P_2 (in Fig. 1) against the beam radius in the afocal subsystem. Solid line is for the cascade system with the designed hybrid lenses and broken line is for the cascade system with the E-FDS3 refractive lenses.

the cascade system. The expected length of the hybridized system is 700 mm, whereas the current system is 1212 mm long. Small footprint may reduce constraints on machine layouts of the cascaded configuration.

To construct the hybrid lens, a plano-convex lens and a diffractive lens can be produced independently and then can be combined by optical contact technique. This kind of binding method, which uses no adhesive, avoids affecting the quality of transmitted pulses. There is no particularly stringent requirement in fabrication of the hybrid lens, except for the focal length of its refractive surface, f_{10}. The error tolerance of f_{10} is expected to be < 1% for sufficiently small chromatic aberrations. Stock lenses usually have focal length errors of 1-2%. The focal length f_{10} should be fixed by prioritizing the chromatic aberration over the pulse front distortion, because the latter is much less sensitive to the focal length error.

The proposed pulse delivery system will be in operation with both temperature and humidity controlled for a stable pulse generation. The optical elements used in the system are made from thermally stable glasses, such as fused silica, which should be transparent over the wavelength range of 780 nm ± 23 nm for 20-fs-pulses.

6 CONCLUSIONS

We have proposed the use of hybrid lenses, instead of refractive lenses, in an achromatic cascade optical system that we developed for multifocusing ultrashort pulse beams. We have realized through numerical analysis that by constructing the afocal subsystem with a pair of hybrid lenses, each composed of a refractive lens and a diffractive lens, spatial and temporal distortions can be compensated for a 20-fs-pulse beam. Using this hybridized cascade system, an ultrashort pulse beam can be multifocused in significantly large array dimensions, say, 5.0 mm across, while high resolutions are accomplished in both space and time. The future work is to fabricate a hybrid lens and validate its effectiveness through experiments with 20-fs-pulses. This pulse delivery system enables high-throughput material-processing using ultrashort-pulsed lasers.

ACKNOWLEDGMENTS

This work was supported by the Amada Foundation under grant AF-2017215.

REFERENCES

Lenzner, M., Kruger, J., Kautek, W., and Krausz, F., “Precision laser ablation of dielectrics in the 10-fs regime,” *Appl. Phys.* A 68, 369–371 (1999).

Chimier, B., Uteza, O., Sanner, N., Sentis, M., Itina, T., Lassonde, P., Legare, F., Vidal, F., and Kieffer, J. C., “Damage and ablation threshold of fused-silica in femtosecond regime,” *Phys. Rev*. B 84, 094104–0941049 (2011).

Amako, J. and Fujii, E., “Beam delivery system with a non-digitized diffractive beam splitter for laser drilling of silicon,” *Optics and Lasers in Eng.* 77, 1–7 (2016) and the references cited therein.

Kuroiwa, Y., Takeshima, N., Narita, Y., Tanaka, S., and Hirao, K., “Arbitrary micropatterning method in femtosecond laser microprocessing using diffractive optical elements,” *Opt. Express* 12, 1908–1915 (2004).

Hayasaki, Y., Sugimoto, T., Takita, A., and Nishida, N., “Variable holographic femtosecond laser processing by use of a spatial light modulator,” *Appl. Phys. Lett.* 87, 031101–031103 (2005).

Kelemen, L., Valkai, S., and Ormos, P., “Parallel photopolymerisation with complex light patterns generated by diffractive optical elements,” *Opt. Express* 15, 14488–14497 (2007).

Sakakura, M., Sawano, T., Shimotsuma, Y., Miura, K., and Hirao, K., “Parallel drawing of multiple bent optical waveguides by using a spatial light modulator,” *Jpn. J. Appl. Phys.* 48, 126507–126511 (2009).

Jesacher, A. and Booth, M. J., “Parallel direct laser writing in three dimensions with spatially dependent aberration correction,” *Opt. Express* 18, 21090–21099 (2010).

Amako, J., Nagasaka, K., and Kazuhiro, N., “Chromatic-distortion compensation in splitting and focusing of femtosecond pulses by use of a pair of diffractive optical elements,” *Opt. Lett.* **27**, 969–971 (2002).

Li, G., Zhou, C., and Dai, E., “Splitting of femtosecond laser pulses by using a Dammann grating and compensating grating,” *J. Opt. Soc. Am.* A 22, 767–772 (2005).

Hasegawa, S. and Hayasaki, Y., “Dynamic control of spatial wavelength dispersion in holographic femtosecond laser processing,” *Opt. Lett.* 39, 478–481 (2014).

Minguez-Vega, G., Lancis, J., Caraquitena, J., Torres-Company, V., and Andres, P., “High spatiotemporal resolution in multifocal processing with femtosecond laser pulses,” *Opt. Lett.* 31, 2631–2633 (2006).

Martinez-Cuenca, R., Mendoza-Yero, O., Alonso, B., Sola, I. J., Minguez-Vega, G., and Lancis, J., “Multibeam second-harmonic generation by spatiotemporal shaping of femtosecond pulses,” *Opt. Lett.* **7**, 957–959 (2012).

Torres-Peiro, S., Gonzalez-Ausejo, J., Mendoza-Yero, O., Minguez-Vega, G., Angres, P., and Lancis, J., “Parallel laser micromachining based on diffractive optical elements with dispersion compensated femtosecond pulses,” *Opt. Express* 21, 31830–31835 (2013).

Amako, J. and Nakano, H., “Distortion-compensated multifocusing of ultrashort pulse beams using cascade optical system,” *Appl. Opt.* 57, 33–41 (2018).

Stone, T. and George, N., “Hybrid diffractive-refractive lenses and achromats,” *Appl. Opt*. 27, 2960–2971 (1988).

Piestun, R., and Miller, D. A. B., “Spatiotemporal control of ultrashort optical pulses by refractive-diffractive-dispersive structured optical elements,” *Opt. Lett.* 26, 1373–1375 (2001).

Hoya's Official Website, http://www.hoya-opticalworld.com/english/datadownload/index.html.

Diels, J.–C.and Rudolph, W., *Ultrashort Laser Pulse Phenomena*, 2nd ed. (Elsevier, 2006), p.10.

Yariv, Y. and Yeh, P., *Optical Waves in Crystals* (John Wiley & Sons, 2003), p.34.

Bor, Z., "Distortion of femtosecond laser pulses in lenses and lens systems," *J. Mod. Opt.* 35, 1907–1918 (1988).

Bor, Z., "Distortion of femtosecond laser pulses in lenses," *Opt. Lett.* 14, 119–121 (1989).

Harm, W., Roider, C., jesacher, A., Bernet, S., and Ritsch-Marte, M., "Dispersion tuning with a varifocal diffractive-refractive hybrid lens," *Opt. Express* 22, 5260-5269 (2014).

SCITEPRESS
SCIENCE AND TECHNOLOGY PUBLICATIONS